

Photoluminescence in deuterated highly doped GaAs(Zn)

P. de Mierry* and M. Stutzmann

Max-Planck-Institut für Festkörperforschung, Heisenbergstrasse 1, D-7000 Stuttgart 80, Federal Republic of Germany

(Received 12 May 1992)

The passivation of Zn acceptors by atomic deuterium in heavily doped *p*-type GaAs is investigated by photoluminescence (PL) and infrared reflectance measurements. A large variation in the optical gap is observed, resulting from changes in the free-hole concentration. A broad PL band in the range 1.30–1.45 eV occurs after deuteration. This band is not related to plasma or radiation damage at the surface, but originates in the bulk of the deuterated layer. Using secondary-ion-mass spectrometry and thermal effusion combined with etch-back experiments, it is demonstrated that a large amount of deuterium ($> 10^{20} \text{ cm}^{-3}$) coexists with the Zn-D complexes in the passivated region, in the form of electrically inactive species.

INTRODUCTION

The passivation of shallow dopants by hydrogen in crystalline semiconductors has been extensively studied during the last decade.¹ Hydrogenation causes a pronounced decrease in the free-carrier concentration, as measured by electrical transport techniques. The simultaneous increase in the carrier mobility argues for the dopant neutralization rather than a classical mechanism of compensation. Infrared (IR) spectroscopy confirmed that the passivation proceeds via the formation of neutral H-dopant entities.

The photoluminescence (PL) technique was successfully applied to study the passivation of shallow dopants, e.g., C acceptors in high-purity *p*-type molecular-beam epitaxy and metal-organic chemical-vapor deposition GaAs,² and Si donors ($\approx 10^{17} \text{ cm}^{-3}$) in Si-implanted liquid-encapsulated Czochralski GaAs.³ After hydrogenation, the intensity of the acceptor bound exciton and band-to-impurity transitions was found to decrease drastically.

The PL technique was also used to detect the presence of H₂-plasma-related defects in crystalline semiconductors. The exact nature of these defects is to date still uncertain. For example, additional PL features were observed in plasma-hydrogenated silicon.⁴ They were attributed to the presence of platelets within the first 100 nm of the exposed surface, consisting of hydrogen aggregates localized in the {111} planes of silicon. This assertion was criticized in a recent paper,⁵ showing that analogous PL bands were detected down to a depth of 500 nm from the surface, in a region where the presence of platelets is improbable. Furthermore, reactive ion etching of silicon, using different plasmas such as H₂, NF₃, CF₄, or O₂, was found to produce identical PL bands. Intrinsic microdefects, identified by cross-sectional transmission electron microscopy (XTEM) over 1 μm depth in plasma-treated silicon, were suspected to provide radiative recombination centers. The role of hydrogen, however, is still controversial since this element is a contaminant in all dry-etching processes.

Plasma-related defects in GaAs have been investigated little. A low-energy band in the PL emission spectrum of Si-doped GaAs was reported after hydrogen plasma exposure.³ This band was associated with the plasma damage near the surface. Arsenic vacancies were the main defect identified after a H₂-plasma treatment.^{6,7}

In the present work, the optical and electrical properties of highly *p*-doped GaAs(Zn), after exposure to a D₂ glow-discharge plasma, are investigated by PL and IR reflectance. The latter method was used to determine the free-hole concentration for the same samples used for PL without the need for electrical contacts.⁸

It is now well established that H (and D) passivate the Zn acceptors in GaAs.⁹ The microscopic structure of H bonding with Zn was determined using IR absorption,¹⁰ and recently, the dissociation energy of the complex has been obtained.¹¹

The PL of highly *p*-doped GaAs has been used to determine one of the main effects of high doping, namely band-gap narrowing.^{12–15} Both exchange and correlation effects in the free-carrier system¹⁶ and carrier-impurity ion interactions¹⁷ contribute to an effective reduction of the energy gap in heavily doped semiconductors. In *p* GaAs the gap shrinkage is a very sensitive function of the free-hole concentration. Since deuteration results in a drastic reduction in the free-hole concentration, a variation (broadening) of the band gap is thus expected. In addition, post-deuteration annealing can be performed to reactivate the dopants. A relationship between the gap narrowing and the hole concentration can thus be obtained without changing the actual concentration of dopant atoms in the lattice. This allows us to separate alloying effects caused by substitutional dopants from purely electronic effects due to the presence of free carriers.

Since we observed that the PL spectra of the deuterated samples exhibited additional features, sequential chemical etching of the surface was performed in order to assess whether this luminescence was due to near-surface plasma damage or bulk effects. This optical investigation was combined with thermal effusion and secondary-ion-mass spectrometry (SIMS) analysis which provided fur-

ther information on the various deuterium bonding configurations in the crystal.

I. EXPERIMENTAL DETAILS

The samples used in this study were single crystals of GaAs with $\langle 100 \rangle$ orientation doped with zinc ($[Zn] = 7 \times 10^{19} \text{ cm}^{-3}$). All the surfaces were mechano-chemically polished in a NaOCl solution to a mirrorlike finish.

The samples were exposed at 170 °C for 20 h to a remote D_2 glow-discharge plasma described elsewhere.¹⁸ A bias voltage of -320 V was applied to the sample holder. Under these conditions, a significant passivation ($> 90\%$) could be achieved.¹⁹

The carrier concentration was obtained by IR reflectance. IR spectra were recorded at room temperature, between 200 and 4000 cm^{-1} , using a Fourier spectrometer. A mirror was used as a reference for the reflection. This method is appropriate for high doping levels, since in that case the IR response is dominated by free-carrier plasma effects.⁸ At the plasma frequency ω_p , the reflectivity R reaches unity, and the carrier concentration N can be obtained from

$$\omega_p^2 = 4\pi Ne^2 / m^* \epsilon_\infty, \quad (1)$$

where e is the electronic charge, m^* is the carrier effective mass, and ϵ_∞ is the optical dielectric constant.

A graphical method was used to determine N : in practice, the frequencies ω were determined at $R = 0.3$. A calibration plot of $\ln(\omega_{R=0.3})$ vs $\ln(N)$ was obtained, using the reflectance data for two samples of known doping levels. This plot is shown in Fig. 1. It was verified that the straight line passing through the experimental points gives the expected square-root dependence of Eq. (1). From this point the carrier density N of a sample can be readily estimated from the IR spectra, without the need for electrical contacts. It should be noted that this determination is valid only in the case of relatively high-doping levels, when the plasma frequency ω_p is high compared to the LO-phonon frequency ω_{LO} , i.e., when the

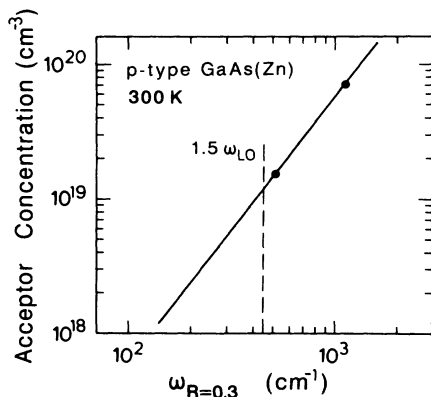


FIG. 1. $\omega_{R=0.3}$ (energy at which IR reflectivity reaches 30%) vs carrier concentration N in p GaAs(Zn) for two samples of known doping concentration. This plot can be used to determine N from $\omega_{R=0.3}$ in the reflectivity curves. ω_{LO} is the longitudinal-optical-phonon frequency (see text).

coupling between the LO-vibrational modes and the longitudinal-collective excitations of plasmons is negligible.²⁰ This condition is fulfilled for $\omega_p > 1.5\omega_{LO}$.²⁰ The dashed line shown in Fig. 1 gives the lower limit for the determination of N by the simplified method described in Fig. 1.

Interference fringes were noticed in the IR spectra of the as-deuterated samples, due to the fairly abrupt profile of free carriers in the passivated region. The thickness d of the passivation region was calculated using the thin-film relation: $\Delta\omega = 1/2nd$, where n is the refractive index and $\Delta\omega$ is the difference in frequency (in units of cm^{-1}) between two successive maxima or minima in the reflection spectra.

In some cases the free-hole profile was determined from a quantitative computer modeling of the IR spectra. Details of the fitting procedure are given in Ref. 21. Annealing treatments after deuteration were carried out in a molecular hydrogen atmosphere.

Etching of the deuterated GaAs surfaces was accomplished in a 486 H_2O : 20 HNO_3 : 7 H_2O_2 solution. The etching rate, evaluated from the changes of the interference fringes in the IR reflectance spectra, was $\approx 0.1 \mu\text{m}/\text{min}$.

The PL was recorded at 77 K, using for excitation the 4764- and 6764-Å lines of a Kr^+ laser. The flux density of the photons incident onto the surface was $\approx 1.2 \times 10^{17} \text{ cm}^{-2} \text{ s}^{-1}$. The luminescence was collected in a direction normal to the surface and focused into the entrance slit of a triple 0.6-m spectrometer (Spex 1877) equipped with 1200 lines/mm holographic gratings. A cooled optical multichannel analyzer (OMA, Princeton Applied Research) was used for detection. The recorded data were corrected for the spectral sensitivity of the detection system through comparison with a calibrated tungsten lamp.

Ellipsometric measurements were performed with a Rotating Analyzer Ellipsometer at room temperature. Details of the technique are described in the literature.^{22,23}

The effusion measurements were obtained by heating the samples inside a quartz tube with a linear temperature ramp ($20^\circ\text{C}/\text{min}$). The residual vacuum prior to heating was $\approx 5 \times 10^{-7} \text{ mbar}$. The outdiffusing deuterium was constantly evacuated with a turbomolecular pump and the D_2 partial pressure was measured using a quadrupole mass spectrometer.

SIMS analysis was performed by a CAMECA IMS4F apparatus, using a primary-ion source of cesium. The absolute deuterium concentration was determined using D-implanted specimen of known D concentration. The estimated error in the D concentration is about 20%. The depth scale was established by measuring the sputter-induced craters with a Talystep stylus profilometer (sensitivity $\approx 200 \text{ \AA}$).

II. RESULTS AND DISCUSSION

A. Evidence for acceptor passivation

Typical PL spectra for Zn-doped p GaAs are shown in Fig. 2. The PL of the reference sample exhibits a single

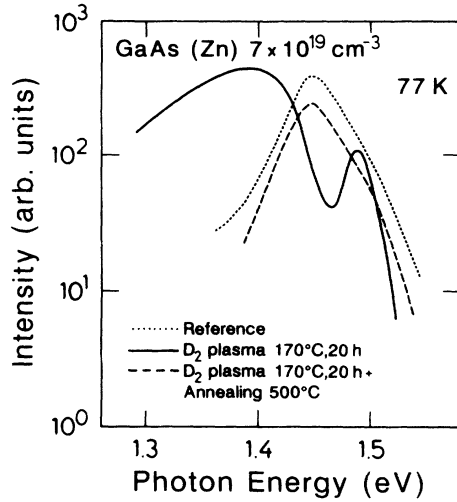


FIG. 2. Typical PL spectra of strongly *p*-type GaAs(Zn) before and after D₂-plasma exposure at 170°C for 20 h. The effect of a subsequent annealing at 500°C for 5 min is also shown. The laser wavelength was 6764 Å.

broad peak. In heavily *p*-doped semiconductors, the Fermi energy E_F lies well below the valence-band edge. The shape of the emission spectrum results from optical transitions connecting the bottom of the conduction band with empty valence-band states above the Fermi energy.

After D₂ exposure, the emission peak is strongly displaced towards high energies, indicating that the optical gap has increased. This effect is related to the reduction of hole concentration, as a result of the passivation of Zn acceptors by deuterium. In addition, a broad shoulder shows up in the low-energy range of the spectrum. Its origin will be discussed in the next section.

Also shown in Fig. 2 is the PL of the same deuterated sample after annealing at 500°C for a few minutes. The spectrum resembles that of the reference sample. At this temperature, all the deuterium was effused and the crystal recovers its initial properties.

Concerning the deuterated crystal, it was noticed that changing the laser wavelength to 4762 Å (2.60 eV) instead of 6764 Å (1.83 eV) increased the overall luminescence by less than a factor 1.5. At higher energies, the exciting beam probes regions closer to the surface and it is likely that, near the surface, a more complete passiva-

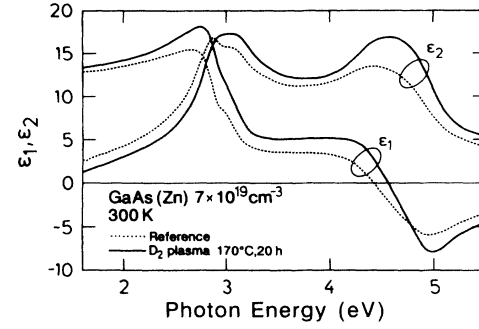


FIG. 3. Real part ϵ_1 and imaginary part ϵ_2 of the dielectric constant vs photon energy in GaAs(Zn).

tion of nonradiative deep centers is achieved, due to the large concentration of deuterium.

The penetration depth probed by the laser beam was determined on the basis of spectroscopic ellipsometry measurements. The results are shown in Fig. 3. The complex dielectric constant was obtained in the range 1.5–6 eV. The spectra display two main features corresponding to the E_1 and E_2 interband optical transitions in GaAs.^{24,25} We draw here attention to the fact that, after plasma exposure, critical features of ϵ_1 and ϵ_2 are shifted to higher energies by about 100 meV, demonstrating the gap increase caused by carrier passivation. The absorption coefficient α was calculated from

$$\alpha = \frac{4\pi k}{\lambda},$$

with

$$k = \left\{ \frac{-\epsilon_1 + \left[\epsilon_1^2 + \epsilon_2^2 \right]^{1/2}}{2} \right\}^{1/2}. \quad (2)$$

The corresponding absorption depths $1/\alpha$ are listed in Table I.

PL spectra of an as-deuterated sample subsequently annealed at 250°C are given in Fig. 4 for different annealing times. Annealing changes the initial spectrum significantly. The emission peak at 1.49 eV broadens towards the low-energy side, whereas the intensity of the band at ≈ 1.35 eV decreases. The shift of the emission

TABLE I. Penetration depth $1/\alpha$ of the laser beam in GaAs(Zn) at two different exciting wavelengths λ_L . ϵ_1 and ϵ_2 were determined from Fig. 3. The extinction coefficient k and the absorption coefficient α were calculated using Eq. (2).

	GaAs reference		GaAs, D ₂ plasma 170°C; 20 h	
	$\lambda_L = 6764$ Å (1.83 eV)	$\lambda_L = 4762$ Å (2.60 eV)	$\lambda_L = 6764$ Å (1.83 eV)	$\lambda_L = 4762$ Å (2.60 eV)
ϵ_1	13.2	15.3	13.7	17.2
ϵ_2	3.6	9.9	2.3	8.0
k	0.48	1.21	0.31	0.94
α (cm ⁻¹)	9.0×10^4	3.2×10^5	5.9×10^4	2.5×10^5
$1/\alpha$ (nm)	110	30	170	40

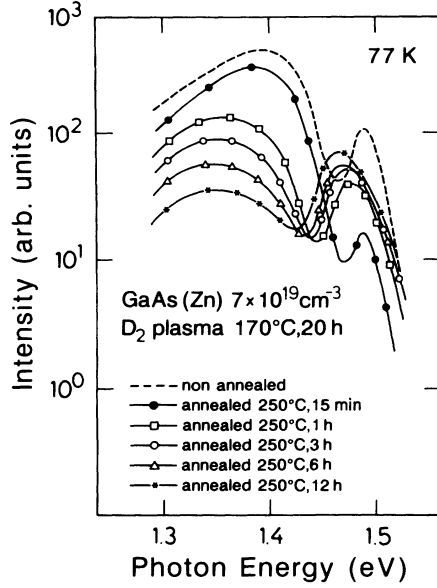


FIG. 4. Effect of isothermal annealing at 250°C on the PL of GaAs(Zn) initially deuterated at 170°C for 20 h. $\lambda_L = 6764 \text{ \AA}$.

peak towards lower energies as the annealing time increases results from a gap shrinkage caused by the thermal reactivation of Zn acceptors.

It should also be noted that, in the early stages of annealing, a drop in the peak intensity was always observed. This effect may be due to the thermal reactivation of passivated nonradiative centers of unknown microscopic nature.

For the sake of clarity, the emission peaks as a function of annealing time are plotted in Fig. 5 on a linear scale and normalized to unity. The direct gap E_G was determined as the intersection of the tangent to the low-energy tail of the emission curve with the background. $E_F + E_G$, i.e., the difference between the minimum of the conduction band and the Fermi level, is also shown (arrows in Fig. 5). E_F was calculated relative to E_V , using the following expression and assuming parabolic bands:

$$p = N_V(T) F_{1/2}(\eta_f) \quad \text{with} \quad \eta_f = \frac{E_F - E_V}{kT}, \quad (3)$$

where

$$F_{1/2} = \frac{2}{\pi^{1/2}} \int_0^\infty \frac{\eta^{1/2}}{1 + \exp(\eta - \eta_f)} d\eta$$

is the Fermi-Dirac integral.²⁶

The free-hole concentration p was determined for each duration of annealing, using IR reflectance measurements. These data, together with the band-gap shrinkage ΔE_G , are listed in Table II.

ΔE_G was expressed by $E_G(\text{pure}) - E_G(\text{doped})$, taking for

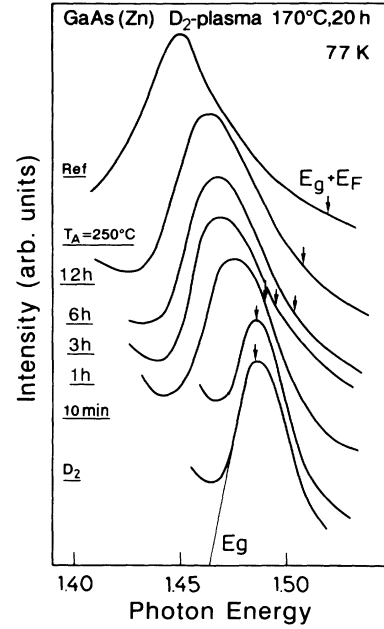


FIG. 5. Evolution of the PL emission peak as a function of annealing time in deuterated GaAs(Zn). E_G and $E_G + E_F$ represent the energy gap and the Fermi energy, respectively. The spectra have been offset vertically for better comparison. $\lambda_L = 6764 \text{ \AA}$.

TABLE II. Free-hole concentration, band gap, and Fermi-level positions as a function of annealing treatment. The free-hole concentration p was measured by IR reflectance; the energy gap E_G was determined from the PL spectra; ΔE_G represents the band-gap narrowing expressed by $\Delta E_G = E_G(\text{pure}) - E_G(\text{doped})$ with $E_G(\text{pure}) = 1.513 \pm 0.03 \text{ eV}$; E_F is the Fermi energy with respect to the valence band, calculated with Eq. (3); $E_F + E_G$ is the Fermi energy as measured from the conduction-band edge. All data were determined at 77 K, except p which was measured at room temperature.

Treatment	$[p]$ (cm^{-3})	E_G (eV)	ΔE_G (meV)	E_F (meV)	$E_G + E_F$ (eV)
D ₂ ; 170°C; 20 h	6×10^{18}	1.464 ± 0.001	44 ± 4	21	1.485 ± 0.001
250°C; 15 min	7.5×10^{18}	1.461 ± 0.001	47 ± 4	25	1.486 ± 0.001
250°C; 1 h	1.8×10^{19}	1.444 ± 0.001	64 ± 4	46	1.490 ± 0.001
250°C; 3 h	2.4×10^{19}	1.439 ± 0.001	69 ± 4	56	1.495 ± 0.001
250°C; 6 h	3.2×10^{19}	1.434 ± 0.001	74 ± 4	69	1.504 ± 0.001
250°C; 12 h	3.8×10^{19}	1.430 ± 0.001	78 ± 4	77	1.508 ± 0.001
Reference	7×10^{19}	1.408 ± 0.001	100 ± 4	111	1.519 ± 0.001

the band gap of pure GaAs at 77 K the value 1.513 ± 0.03 eV, deduced from Thurmond's relation:²⁷

$$E(T) = E(0) - \frac{\alpha T^2}{\beta + T}$$

with

$$\alpha = (5.405 \pm 0.25) \times 10^{-4} \text{ eV K}^{-1},$$

$$\beta = (204 \pm 45) \text{ K},$$

and

$$E_G(0) = (1.519 \pm 0.001) \text{ eV}.$$

We present in Fig. 6 a plot of the band-gap shrinkage ΔE_G versus hole concentration. The experimental points of Olego and Cardona¹⁴ for Zn-doped GaAs of different doping levels are also added. An empirical relation for the gap shrinkage can be deduced:

$$\Delta E_G = 2.34 \times 10^{-5} p^{1/3}$$

with ΔE_G in eV and p in cm^{-3} . Casey and Stern²⁸ obtained a similar relation by comparing their calculated absorption coefficient curves with the corresponding experimental curves and finding the energy shift which gave the best fit. In the range $1 \times 10^{18} - 2 \times 10^{19} \text{ cm}^{-3}$ the concentration dependence of the energy gap at room temperature was expressed as

$$\Delta E_G = 1.6 \times 10^{-5} p^{1/3}.$$

A somewhat larger gap shrinkage was reported by Borghs *et al.*,¹⁵ from PL measurements at 30 K on GaAs(Zn) doped in the range $3 \times 10^{17} - 3 \times 10^{18} \text{ cm}^{-3}$:

$$\Delta E_G = 2.6 \times 10^{-5} p^{1/3}.$$

In Fig. 7, we have plotted the experimental points for E_M (the luminescence maximum) and $E_G + E_F$ of the PL emission peak, as a function of doping, along with the points of Cusano,¹² Pankove,¹³ as well as Olego and Cardona.¹⁴ All sets of data agree well. In the studies reported so far in the literature, the carrier density is varied by

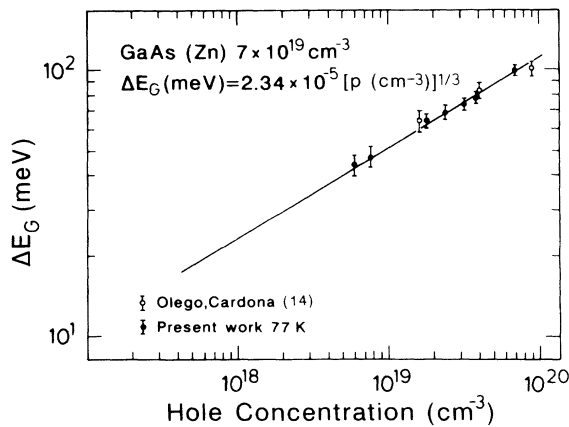


FIG. 6. Hole concentration dependence of the band-gap shrinkage. Open symbols are from Ref. 14 and correspond to ΔE_G extrapolated to 0 K.

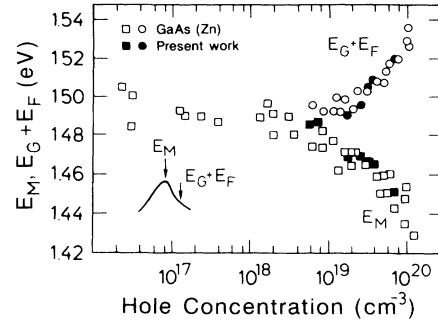


FIG. 7. Luminescence peak maximum E_M , and Fermi energy $E_G + E_F$ in plasma-passivated GaAs(Zn), as a function of hole concentration, compared to various data taken from the literature (Refs. 12–14) for GaAs(Zn) with varying doping levels (open symbols).

changing the doping level. Our results demonstrate that the major contribution to the band-gap variation in Zn-doped GaAs comes indeed from the change in the free-hole concentration, since the actual dopant concentration is not modified by deuteration.

B. Other deuterium bonding configurations

1. Photoluminescence measurements

In the preceding part, the passivation of acceptors by atomic deuterium was studied by following the energy position of the high-energy luminescence peak for different annealing times. Good agreement was found with the literature data, obtained for GaAs crystals of various doping levels. In this section, we investigate the additional optical changes induced by deuteration.

After plasma exposure, the PL spectra exhibit a broad shoulder in the range 1.30–1.45 eV (Fig. 2). This feature progressively vanishes by thermal annealing at 250 °C (Fig. 4).

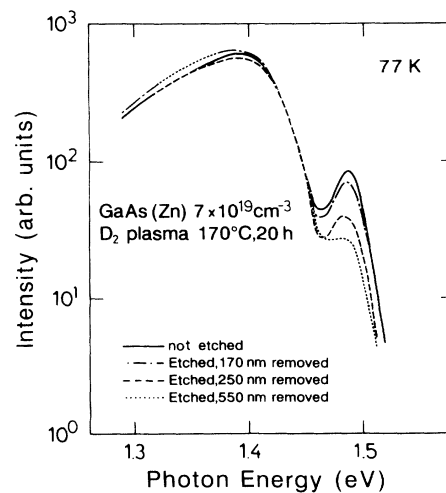


FIG. 8. Effect of etching on the PL of a passivated GaAs(Zn) sample. The thickness of the initially passivated region was 1700 nm. $\lambda_L = 6764 \text{ \AA}$.

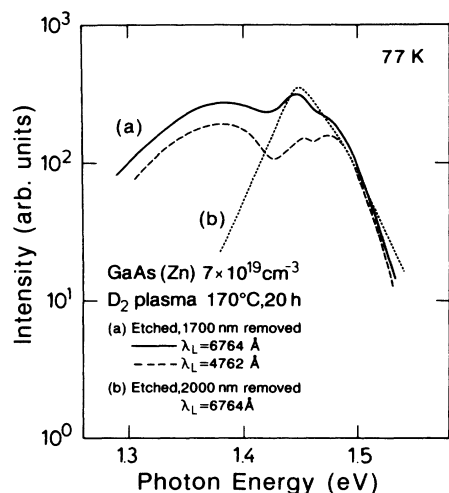


FIG. 9. PL spectra of the sample in Fig. 8, after removal of a layer of (a) ≈ 1700 nm depth and (b) ≈ 2000 nm depth by chemical etching.

The GaAs surfaces were chemically etched to assess whether this low-energy band originates from the bulk or the surface of the deuterated sample. The results are shown in Fig. 8. The passivated depth of the starting material is 1700 nm. After removing 550 nm from the surface, the low-energy band still remains unchanged. It is hence not related to the deuterium plasma damage as this damage is located near the surface, to a depth of 200 nm at most.

In addition, the sharp emission peak at 1.49 eV progressively decreases. This drop is tentatively explained by a higher fraction of nonpassivated recombination centers in the bulk.

The surface of the same sample was further etched, until the remaining passivated layer reached a thickness of a few ten nanometers. Figure 9 displays the PL spectra, obtained at two excitation wavelengths, corresponding to different regions probed by the laser beam (see Table I). At $\lambda_{\text{exc}} = 4762$ Å, an additional peak at 1.45 eV shows up, indicating that the nondeuterated region beyond the passivated layer now contributes to the overall luminescence. This contribution becomes even more important at a lower laser excitation energy ($\lambda_{\text{exc}} = 6764$ Å), when light penetrates deeper into the crystal.

The low-energy band is still clearly observed, confirming that this luminescence originates in the deuterated bulk. The luminescence characteristic of the non-D samples was finally recovered, after that the whole deuterated region was removed (curve *b* in Fig. 9).

2. Thermal-effusion measurements

The thermal effusion of deuterium out of GaAs(Zn) was used to obtain further information about the origin of the low-energy band seen in photoluminescence. For this purpose, a series of deuterated samples underwent the same post-plasma treatments as those used in the PL studies.

Figure 10 shows the development of the effusion spec-

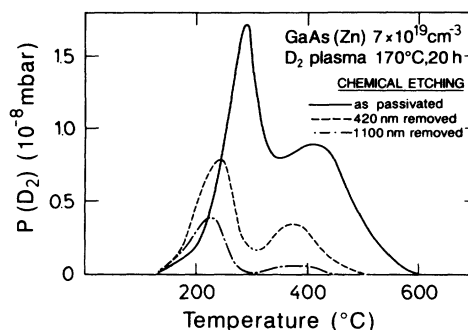


FIG. 10. Influence of etching on the deuterium effusion spectra of GaAs(Zn) deuterated at 170°C for 20 h.

tra as successive layers of GaAs are removed by chemical etching. The as-deuterated sample exhibits two effusion peaks, a sharp effusion maximum at $\approx 300^\circ\text{C}$ and a broader peak at $\approx 420^\circ\text{C}$, characteristic of at least two bonding configurations with different binding energies. After etching, the samples conserve the same two-peak structure. In addition, the peaks are shifted to somewhat lower temperatures. One possibility is that this shift is due to a lower desorption activation energy of D_2 molecules induced by the surface chemical etching. Alternatively, diffusion of deuterium towards the surface may be a rate-limiting step in the desorption process.

The effects of a 250°C annealing treatment on the effusion of deuterium in GaAs(Zn) are shown in Fig. 11. The main observation is the disappearance of the low-temperature (LT) peak after annealing for 15 min. This treatment has already been shown to slightly alter the PL (Fig. 4) and hole concentration (Table II). A quantitative comparison of these experimental results leads us to invoke the presence of excess deuterium, i.e., D not involved in the complex Zn-D or in the low-energy PL band, to explain the LT effusion peak.

After the initial annealing step, the effusion peak at 420°C then decreases as a function of annealing time. This peak is believed to be mainly due to the dissociation of Zn-D complexes deep in the passivated layer. This assignment is substantiated by the following quantitative

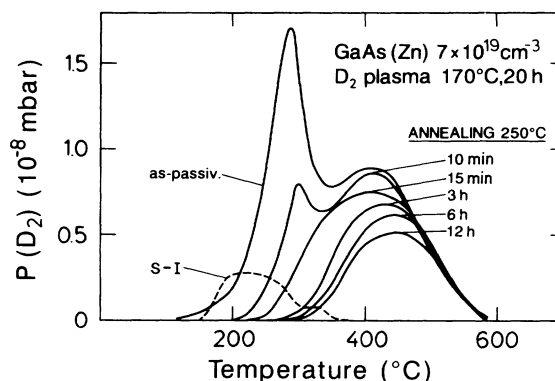


FIG. 11. D_2 effusion spectra of GaAs(Zn) deuterated at 70°C for 20 h and annealed at 250°C for various times. The effusion from semi-insulating (100)GaAs (*S-I*) is also shown.

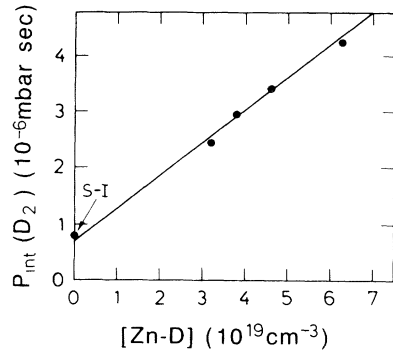


FIG. 12. Relation between the amount of deuterium contained in the annealed samples (integral of the effusion spectra in Fig. 11) and the concentration of Zn-D complexes.

analysis: First, the effusion spectrum seen in Fig. 11, for a deuterated undoped single crystal of GaAs, does not exhibit the peak at 420°C. Secondly, as shown in Fig. 12, we find a linear relation between the total amount of deuterium in the crystal (integral of the effusion curves), and the remaining concentration of Zn-D complexes, obtained by $[Zn-D] = [Zn] - p$, where p takes the values listed in Table II, and $[Zn] = 7 \times 10^{19} \text{ cm}^{-3}$.

3. SIMS measurements

The distribution of deuterium in GaAs(Zn) was determined by SIMS for a sample etched over a depth of ≈ 400 nm immediately after plasma exposure. The resulting D profile shown in Fig. 13 exhibits a fairly pronounced step-like shape, characteristic of a trap-limited diffusion.^{8,29} Also included in the figure is the profile of Zn-D complexes obtained from a modeling of the IR reflectance spectrum. The passivated layer closely matches the deuterated region. The drop in the Zn-D profile coincides with the decrease of D with however a slight discrepancy which is related to the uncertainty inherent in the SIMS measurements or the analysis of the IR spectra. This again indicates that the diffusion of atomic deuterium in GaAs(Zn) at the plasma temperature of 170°C is dominated by trapping on the dopant atoms. It is remarkable

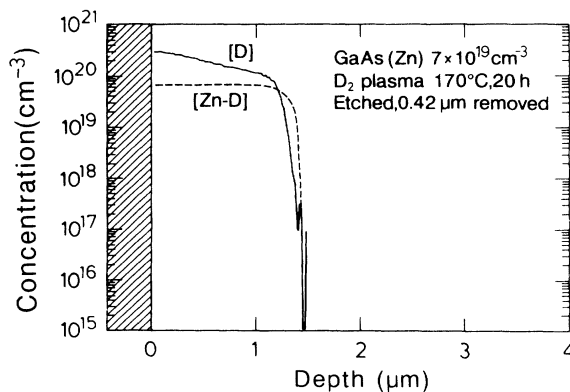


FIG. 13. SIMS profile of deuterium, and concentration profile of Zn-D complexes deduced from IR reflectance, in a deuterated GaAs(Zn) sample after removal of a 0.42- μm surface layer (hatched area).

that within the plateau region, the total D content exceeds the Zn-D density by about a factor of 2. The excess deuterium approaches a few 10^{20} cm^{-3} and should be even larger for a nonetched sample when the diffusion profile is extrapolated to the surface.

The effects of a short-time annealing (250°C; 10 min) on the passivation efficiency in deuterated GaAs(Zn) are illustrated in Fig. 14. The Zn-D profiles were again deduced from a modeling of the reflectance spectra. It appears that after annealing, the depth of the passivated region is increased by several thousand Å. In addition, a small fraction of Zn-D complexes are dissociated (dashed curve in Fig. 14). These results suggest that upon annealing, deuterium atoms are released from the complexes and diffuse deeper in the bulk, where secondary trapping on Zn atoms occurs. However, the fact that the total amount of passivating deuterium (integral of the curves) is significantly larger after annealing clearly indicates that an excess of inactive deuterium initially present in the as-passivated sample was involved in the diffusion and trapping processes, too.

The annealed sample in Fig. 14 was analyzed by SIMS to determine the depth distribution of D. The resulting D profile shown in Fig. 15 exhibits a plateau-like shape up to $\approx 2 \mu\text{m}$ depth, followed by a diffusion tail extending beyond 4 μm depth. It is noticeable that the deuterated region is now much larger than the passivated depth. It implies that the trapping effect was not dominant during the annealing process. This is explained by the fairly high temperature of annealing (250°C) which changes the diffusion from trap-limited to a more normal mechanism. Nevertheless, it is surprising that this mechanism does not result in a smooth decay of the Zn-D profile at the passivation front. This apparent contradiction can be removed if we consider that the sample was heated from ambient to 250°C with a noninstantaneous temperature rise. Consequently, the trapping contribution should be important within this period.

In a region from the surface up to $\approx 1 \mu\text{m}$ depth, the D profile is curved downward, attesting that deuterium was effused during the annealing treatment. From a comparison with the effusion spectra in Fig. 11 we can unambiguously correlate this out-diffusion with the LT peak occurring at $\approx 300^\circ\text{C}$.

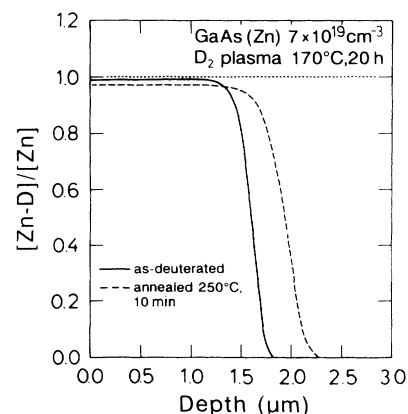


FIG. 14. Effect of a short-time annealing on the Zn-D profiles of deuterated GaAs(Zn) as deduced from IR reflectance.

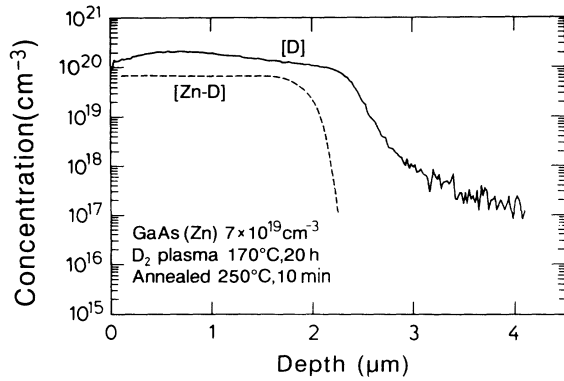


FIG. 15. D (from SIMS) and Zn-D profiles (from IR reflectance) in a deuterated GaAs(Zn) sample subsequently annealed at 250°C for 10 min.

C. Origin of the low-energy PL band

The transition observed in the PL spectra in the range 1.3–1.45 eV is too broad to be associated with hydrogenic centers and must be referred to as complex centers. The persistence of these centers after etching of the surface over a few hundred nanometers excludes the involvement of plasma or radiation damage. On the other hand, it is clear that these centers are closely related to the presence of deuterium in GaAs.

It has been recently proposed⁴ that high concentrations of hydrogen or deuterium ($\approx 2 \times 10^{18} \text{ cm}^{-3}$) in single-crystal silicon could be responsible for additional radiative centers. The defect photoluminescence was attributed to hydrogen-stabilized platelets located within the first 100 nm. In Ref. 4, the authors notice that the observed PL needs not arise from anything else except for hydrogen platelets and that the presence of intrinsic defects or impurities in silicon is not a prerequisite. From our SIMS investigations shown in Figs. 13 and 15, it was established that a substantial excess of deuterium in the form of electrically nonactive (nonpassivating) species was introduced by plasma charging. The presence of H platelike aggregates in GaAs has been ascertained by XTEM measurements.³⁰

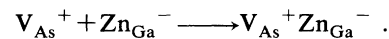
Nevertheless, we would like to mention some possible D interactions with various intrinsic defects expected to be present in melt-grown GaAs single crystals. A number of deep centers revealed by deep-level transient spectroscopy are passivated by atomic deuterium or hydrogen.^{31–33} These centers are due to the presence of point defects (vacancies and interstitials) and, except for the *EL2* level which has been related to an antisite As_{Ga} defect or its complex,³⁴ their exact microscopic structure is still unknown. Some of them are nonradiative and their passivation is usually accompanied by a strong increase in the overall luminescence intensity.³⁵ In our investigations the decrease in the PL emission peak at 1.49 eV in the early stage of annealing or after etching (Figs. 4 and 8) may be due to the reactivation or removal of passivated deep centers inside the crystal.

The role of dislocations in as-grown crystals, produced by plastic deformation during crystal growth, has also been investigated by space- and time-resolved photo-

luminescence.^{36,37} Grown-in dislocations as well as their glide traces in Si-doped LEC GaAs are found to yield lower luminescence intensities than the crystal matrix.³⁶ PL maps of In-alloyed GaAs show different features consisting in dark regions at the center of dislocation clusters surrounded by circular bright areas.³⁷ From the above results, there are many indications that impurities and/or defects getter by dislocations play an important role in the recombining activity of dislocations. This is probably the reason why the interaction of deuterium or hydrogen with dislocations in GaAs remains a matter of debate. Recently, a dopant-dependent interaction was reported in ion-implanted-annealed GaAs.³⁸ In semi-insulating GaAs, there is no definitive evidence for the passivation of dislocations in plastically deformed samples.^{35,39}

The broad PL band reported in the present work is clearly related to the presence of deuterium inside the sample. The segregation of D clusters at dislocations could account for radiative centers in the band gap. This assumption is at present quite speculative. A systematic XTEM investigation should provide useful information on the possible generation and repartition of secondary defects induced by deuteration.

It should be noted that a similar band, centered at 1.37 eV, was reported on melt-grown Zn-doped GaAs samples.⁴⁰ This band was attributed to arsenic vacancy-Zn acceptor ($V_{\text{As}}^+ \text{Zn}_{\text{Ga}}^-$) centers present as native defects in the material. Arsenic vacancies can otherwise be formed by electron irradiation at $E > 250 \text{ KeV}$.⁴¹ It seems thus unlikely that such defects may be created beyond the damage region in our specimen during plasma exposure. However, it is now well established^{6,7} that high concentrations of As vacancies are provided by the D_2 -plasma treatment in the near-surface region. Under plasma exposure at 170°C, radiation-induced arsenic vacancies could diffuse into the bulk to form $V_{\text{As}}^+ \text{Zn}_{\text{Ga}}^-$ complexes as described by the reaction



This mechanism is consistent with the small migration energy of about 1 eV for the As vacancy in GaAs.⁴² Moreover, the diffusion of positively charged As vacancies should be enhanced by a drift effect due to the built-in field within the passivation front.

A similar behavior was observed in electron-irradiated GaAs(Zn) samples.⁴³ A strong increase in the 1.37-eV emission band (factor 200) was reported after thermal annealing at moderate temperatures, in the range 100–200°C. This was attributed to the capture of radiation-induced mobile As vacancies by nearby Zn atoms on Ga sites.

Furthermore, the annealing temperature associated with the breakup of $V_{\text{As}}^+ \text{Zn}_{\text{Ga}}^-$ complexes was found to be 250°C, which corresponds precisely to the decrease of the PL band reported in this study.

One, therefore, has to consider the possibility that at least a certain fraction of Zn-D complexes in GaAs are formed in a different way than assumed at present. Vacancies created by plasma damage at the surface of the crystal can also diffuse into the bulk and form complexes with dopant atoms. After these complexes are formed,

they can react with diffusing H or D atoms, thus giving rise to complexes which could account for the excess deuterium in the passivated region as well as for the low-energy PL band. Further investigations will be necessary to clarify this point.

CONCLUSION

We have confirmed by PL and IR reflectance measurements the efficient passivation of Zn acceptors by deuterium in heavily *p*-doped GaAs. A noticeable energy-gap variation is associated with this passivation. A quantitative relationship between the band-gap shrinkage and the free-hole concentration was obtained, which agrees well with earlier studies using varying doping levels.

After D₂-plasma exposure, the crystal exhibits a strong luminescence band in the range 1.30–145 eV, originating in the bulk. The D distribution and carrier profile, determined by SIMS and IR reflectance, are very similar. This demonstrates a strongly trap-limited diffusion, due to the high-dopant concentration and the fairly low plasma temperature (170°C). In addition, the overall D concentration in the passivated region exceeds the dopant density by about a factor of 2.

Short-time (<15-min) annealing at 250°C does not significantly change the PL spectra or the Zn-D complex density. On the other hand, it is demonstrated that a substantial excess of deuterium diffuses deeper into the bulk, leading to a larger passivation depth. A deuterium-depleted region within the first micrometer of the annealed GaAs surface indicates that D also

outdiffuses during the annealing. This effusion process is associated with the low-temperature peak seen in the effusion spectra. The high concentrations of deuterium, present as electrically inactive species in the crystal matrix could create radiative centers accounting for the broad PL band.

Based on earlier PL studies⁴³ on electron-irradiated GaAs(Zn), the formation of $V_{As}^{+}Zn_{Ga}^{-}$ complexes during plasma exposure may also be invoked to explain the PL band. Arsenic vacancies created by plasma radiation beneath the surface could readily diffuse into the bulk and be trapped by Coulombic attraction with negatively charged Zn atoms. The small migration energy for V_{As}^{+} allied with a drift effect due to the electric field in the passivation front renders the above mechanism plausible. Also, the decrease of the PL band intensity after heat treatment at 250°C for times larger than 15 min is in good agreement with the thermal dissociation of the $V_{As}^{+}Zn_{Ga}^{-}$ centers.⁴³

ACKNOWLEDGMENTS

The authors wish to thank C. Grattapain and B. Theys for performing the SIMS measurements, C. Herrero for the modeling of the infrared reflectance spectra, and P. G. Etchegoin for performing the ellipsometry measurements. One of us (P.M.) acknowledges financial support by the Max-Planck society and the Centre National de la Recherche Scientifique. We thank J. Weber for a critical reading of the manuscript.

*On leave of absence from the CNRS, Laboratoire de Physique des Solides, 1, place A. Briand, 92195 Meudon CEDEX, France.

¹S. M. Myers, M. I. Baskes, H. K. Birnbaum, J. W. Corbett, G. G. Deleo, S. K. Estreicher, E. E. Haller, P. Jena, N. M. Johnson, R. Kirchheim, S. J. Pearton, and M. J. Stavola, *Rev. Mod. Phys.* **64**, 559 (1992).

²N. Pan, S. S. Bose, M. H. Kim, G. E. Stillman, F. Chambers, G. Devanne, C. R. Ito, and M. Feng, *Appl. Phys. Lett.* **51**, 596 (1987).

³J. Weber, S. J. Pearton, and W. C. Dautremont-Smith, *Appl. Phys. Lett.* **49**, 1181 (1986).

⁴N. M. Johnson, F. A. Ponce, R. A. Street, and R. J. Nemanich, *Phys. Rev. B* **35**, 4166 (1987).

⁵J. Weber, *Physica B* **170**, 201 (1991).

⁶P. Friedel, P. K. Larsen, S. Gourrier, J. P. Cabanie, and W. M. Gerits, *J. Vac. Sci. Technol. B* **2**, 675 (1984).

⁷K. C. Hsieh, M. S. Feng, G. E. Stillman, N. Holonyak, Jr., C. R. Ito, and M. Feng, *Appl. Phys. Lett.* **54**, 341 (1989).

⁸C. P. Herrero, M. Stutzmann, A. Breitschwerdt, and P. V. Santos, *Phys. Rev. B* **41**, 1054 (1990).

⁹N. M. Johnson, R. D. Burnham, R. A. Street, and R. L. Thornton, *Phys. Rev. B* **33**, 1102 (1986).

¹⁰B. Pajot, A. Jalil, J. Chevallier, and R. Azoulay, *Semicond. Sci. Technol.* **2**, 305 (1987).

¹¹A. W. R. Leitch, Th. Prescha, and M. Stutzmann, *Appl. Surf. Sci.* **50**, 390 (1991).

¹²D. A. Cusano, *Solid State Commun.* **2**, 353 (1964); D. A. Cusano, *Appl. Phys. Lett.* **7**, 151 (1965).

¹³J. I. Pankove, *J. Phys. Soc. Jpn.* **21**, 298 (1966).

¹⁴D. Olego and M. Cardona, *Phys. Rev. B* **22**, 886 (1980).

¹⁵G. Borghs, K. Bhattacharyya, K. Deneffe, P. van Mieghem, and R. Mertens, *J. Appl. Phys.* **66**, 4381 (1989).

¹⁶M. Combescot and P. Nozieres, *J. Phys. C* **5**, 2369 (1972).

¹⁷P. R. Rimbey and G. D. Mahan, *Phys. Rev. B* **10**, 3419 (1974).

¹⁸C. P. Herrero, M. Stutzmann, and A. Breitschwerdt, in *Impurities, Defects and Diffusion in Semiconductors: Bulk and Layered Structures*, edited by J. Bernholc, E. E. Haller, and D. J. Wolford, MRS Symposium Proceedings No. 163 (Material Research Society, Pittsburgh, 1990), p. 395.

¹⁹M. Stutzmann, J. B. Chevrier, C. P. Herrero, and A. Breitschwerdt, *Appl. Phys. A* **53**, 47 (1991).

²⁰H. R. Chandrasekhar and A. K. Ramdas, *Phys. Rev. B* **21**, 1511 (1980).

²¹G. K. Hubler, P. R. Malmberg, C. N. Waddell, W. G. Spitzer, and J. E. Fredrickson, *Radiat. Effects* **60**, 35 (1982).

²²D. E. Aspnes and A. A. Studna, *Rev. Sci. Instrum.* **49**, 292 (1978).

²³R. M. A. Azzam and N. M. Bashara, *Ellipsometry and Polarized Light* (North-Holland, Amsterdam, 1977).

²⁴P. Lautenschlager, M. Garriga, S. Logothetidis, and M. Cardona, *Phys. Rev. B* **35**, 9174 (1987).

²⁵D. E. Aspnes and A. A. Studna, *Phys. Rev. B* **27**, 985 (1983).

²⁶J. S. Blackmore, *Semiconductor Statistics* (Pergamon, Oxford, 1962), Appendix B.

²⁷C. D. Thurmond, *J. Electrochem. Soc.* **122**, 1133 (1975).

²⁸H. C. Casey and F. Stern, *J. Appl. Phys.* **47**, 631 (1976).

²⁹R. Rizk, P. de Mierry, D. Ballutaud, M. Aucouturier, and D.

- Mathiot, Phys. Rev. B **44**, 6141 (1991).
- ³⁰J. H. Neethling, H. C. Snyman, and C. A. B. Ball, J. Appl. Phys. **63**, 704 (1988).
- ³¹A. Jalil, A. Heurtel, Y. Marfaing, and J. Chevallier, J. Appl. Phys. **66**, 5854 (1989).
- ³²S. J. Pearton and A. J. Tavendale, Electron. Lett. **18**, 715 (1982).
- ³³J. Lagovski, M. Kaminska, J. M. Parsey, Jr., H. C. Gatos, and M. Lichtensteiger, Appl. Phys. Lett. **41**, 1018 (1982).
- ³⁴H. J. von Bardeleben and D. Stievenard, in *Defects in Electronic Materials*, edited by M. Stavola, S. J. Pearton, and G. Davies, MRS Symposium Proceeding No. 104 (Material Research Society, Pittsburgh, 1988), p. 351.
- ³⁵E. M. Omeljanovsky, A. V. Pakhomov, and A. Y. Polyakov, J. Electron. Mater. **18**, 659 (1989).
- ³⁶E. P. Visser, P. J. van der Wel, J. L. Weyher, and L. J. Giling, J. Appl. Phys. **68**, 4242 (1990).
- ³⁷Matthew B. Johnson, A. T. Hunter, and T. C. McGill, in *Defects in Electronic Materials* (Ref. 34), p. 415.
- ³⁸D. K. Sadana, J. P. de Souza, E. D. Marshall, H. Baratte, and F. Cardone, Appl. Phys. Lett. **58**, 385 (1991).
- ³⁹A. Djemel, J. Castaing, and J. Chevallier, Rev. Phys. Appl. **23**, 1337 (1988).
- ⁴⁰C. J. Hwang, Phys. Rev. **180**, 827 (1969).
- ⁴¹D. Pons and J. C. Bourgoin, J. Phys. C **18**, 3839 (1985).
- ⁴²H. R. Potts and G. L. Pearson, J. Appl. Phys. **37**, 2098 (1966).
- ⁴³K. D. Glinchuk, A. V. Prokhorovich, and N. S. Zayats, Phys. Status Solidi **83**, 625 (1984).